Conductance and transparence of long molecular wires

M. Magoga and C. Joachim

CEMES-CNRS, 29 Rue J. Marvig, Boîte Postale 4347, 31055 Toulouse Cedex, France
(Received 10 March 1997)

Electron tunneling through a molecular wire is studied as a function of the length and chemical structure of the molecule. The current intensity is calculated using the electron-scattering quantum-chemistry technique, the wire being connected at both ends to a planar metal-vacuum-metal nanojunction. The tunnel channels and the stepped $I(V)$ characteristics are discussed in detail for the oligo (thiophene ethynylene) molecular wire. At low bias voltage, the conductance G of a metal-molecular wire-metal junction follows a $G = G_0 e^{-\gamma L}$ law with L the interelectrode separation. The inverse damping length γ depends on the internal wire electronic structure and the contact conductance G_0 on the electrode-wire end interactions. Both γ and G_0 can be optimized by changing the chemical structure of the wire, and are given for a large number of oligomers. [S0163-1829(97)06832-X]

I. INTRODUCTION

A single C_{60} molecule or a single chain of Xe atoms is able to close an electric circuit, as demonstrated experimentally using a scanning tunneling microscope (STM).[1,2] In such experiments the relation between the bias voltage V across the STM junction and the current intensity I measured in the macroscopic part of the circuit, is linear for small V.[3] This is obtained by approaching the tip apex beyond the van der Waals mechanical contact region to minimize the contact resistances and thus to eliminate the Coulomb blockade effect.[4]

At low voltage and along the circuit, two different transport regimes contribute to this linearity: the well-known Boltzmann regime in the macroscopic part of the circuit, and a tunneling regime in the STM junction part.[2] This tunneling transport regime exists in the junction because the electronic coupling between the adsorbed molecule and the metal surface enlarges the width of the molecular levels.[3,5] This increases the density of states between these molecular states with the opening of a tunneling channel per enlarged molecular level. At low voltage it is the superposition of all these channels which controls the tunnel characteristics of the junction, although the transport phenomenon remains out off resonance.[1,2]

To investigate further the tunnel transport regime, long and effective molecular or atomic wires must be fabricated. The only criterion found in the literature for selecting a molecule to be a wire is a strong delocalization of its electronic state along one direction. Following this idea, many authors have proposed molecular wires composed of repeated units (oligomers) and tried to synthesize them by controlling the number of units added per stage.[6–12] But questions remain about this abundant list of molecules, for example: How is a given single oligomer connected electrically to the pads? Can a given conjugated oligomer show better conductance than another one of the different chemical structure?

In the following, from all the molecular wires of definite length proposed in the literature, the most representative families are studied (see Table I). These wires are classified not by their intuitive electronic delocalization properties but using two characteristic parameters: the inverse damping length γ and the prefactor G_0 related to the contact conductance. With these two parameters and at low bias voltage, the exponential law

$$G = G_0 e^{-\gamma L} \tag{1}$$

TABLE I. The list of molecular wires studied with their principal characteristics. The damping factor γ, the prefactor G_0, and an evaluation of the tunnel current intensity at 0.1 V for a pad-pad distance of 80 Å are provided.
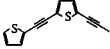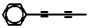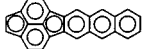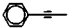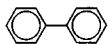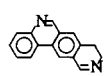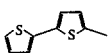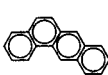
Molecular wire unit	γ (Å^{-1})	G_0 (10^{-9})	I (A)	E_g (eV)
Polyenes	0.187	124	40×10^{-16}	1.11
Oligo(thiophene butadiyne)	0.230	7.6	7.7×10^{-18}	1.25
Oligo(thiophene ethynylene)	0.246	5.5	1.5×10^{-18}	1.22
Oligo(phenyl-butadiyne)	0.267	3.92	2×10^{-19}	1.75
Oligo(cyclopenta-naphto-fluoranthene)	0.270	127	5.3×10^{-18}	1.24
Oligo(phenyl-ethynylene)	0.278	3.06	6.7×10^{-20}	1.74

TABLE I. *(Continued).*

Molecular wire unit	γ (Å^{-1})	G_0 (10^{-9})	I (A)	E_g (eV)
Oligo(phenyl)s	0.281	10.8	18×10^{-20}	1.64
Oligo(pyrido-phenantridine)	0.287	14.0	15×10^{-20}	1.01
Oligothiophenes	0.329	9.6	3.5×10^{-20}	1.53
Oligo(benzo-anthracene)	0.395	41.3	7.8×10^{-23}	1.56

(a)

(b) and (c)

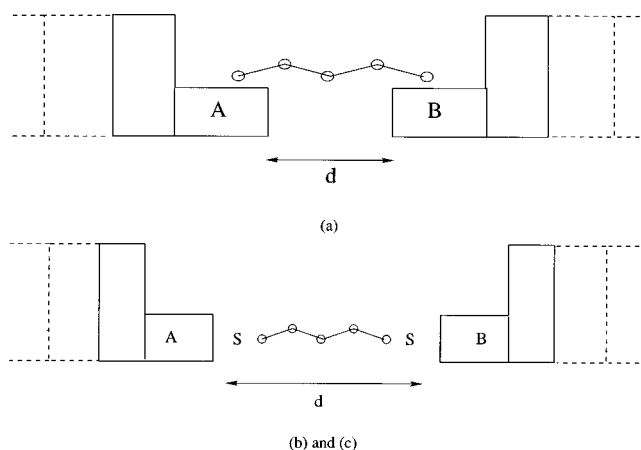FIG. 1. The two configurations of the junction are considered. In case (a) the molecule is adsorbed above the pads, while in case (b) [(c)] the molecule is adsorbed in front of the pads, without (with) a sulfur atom between the wire and the pads to reduce the contact resistance.

of the elastic conductance G of the pad-molecular wire-pad junction as a function of the wire length L can be recovered.[13,14]

In Sec. II, the pad-molecule-pad junction structure is described and the method to calculate Eq. (1) is presented, taking into account all the valence states of the molecule. In Sec. III, the oligo(thiophene ethynylene) molecule is studied, analyzing in detail the decomposition of the junction conductance in tunneling channels. In Sec. IV, we discuss what controls the damping factor γ and the prefactor G_0 by analyzing their variations while changing the chemical nature of the wire, and its position on the junction.

II. TUNNEL CURRENT THROUGH A MOLECULAR WIRE

The measurement of a current through a molecule can be performed with three different experimental setups: a metal-insulator-metal (MIM) junction made of two face-to-face metal electrodes separated by some layers of molecules, a molecule adsorbed on a surface and electrically addressed by a STM tip, or a planar MIM (PMIM) junction made of two separated nanoelectrodes connected by a molecule. Earlier measurements were performed with macroscopic MIM junctions.[15] But in this case, the current flows through the entire molecular film embedded between the electrodes and not through a specific molecule. Since the macroscopic law of association of resistances in parallel is no longer valid at the nanoscale,[16] it is difficult by measuring such a MIM junction to extract the conductance properties of a single molecule only. Notice that the same problem also occurs when reducing the size of one electrode to the size of a metal cluster.[17] If more than one molecule is connected to this cluster, the evaluation of the resistance of one molecule from

the resistance of the aggregate will require lengthy calculations. The STM technique reduces the connecting problem on a small molecule or a single atom by positioning the tip apex above the adsorbate to be connected electrically.[1] But maintaining a 10-nm-long oligomer isolated on a surface and perpendicular to this surface is still a formidable synthetic and surface chemistry task.

The PMIM-like experiment was recently inaugurated by Sander *et al.*, who succeeded in addressing a single carbon nanotube with an interelectrode separation of 140 nm.[4] The transport regime through the nanotube is almost ballistic since it has a negligible HOMO-LUMO gap[18] below 1 meV (HOMO is highest-occupied molecular orbital, and LUMO is the lowest unoccupied molecular orbital). But to study the tunnel transport regime, an oligomer of well-defined length with a non-negligible HOMO-LUMO gap is needed. For the molecular wires listed in Table I, a PMIM junction configuration will be considered here with an interelectrode distance smaller than 10 nm. Progress in the technology permit one to fabricate PMIM nanojunctions with an interelectrode separation down to 8 nm.[19]

The PMIM junction configuration used to calculate the tunnel current intensity of the oligomers in Table I is described in Fig. 1. It consists of two gold pads described atom by atom separated by a gap of variable length. The oligomer will be either chemisorbed or physisorbed across this gap. The current intensity will be calculated away from the pad-molecule-pad junction to recover a ballistic regime of transport in the bulk. In the molecule, the transport regime is clearly a tunnel regime. One reason is that all the selected oligomers have a HOMO-LUMO gap close to or larger than 1 eV. The second reason is that for a standard metal electrode like gold or copper used in technology, the E_f Fermi level is located in the HOMO-LUMO gap of the molecule. The third reason is that we are only interested here in a linear transport regime obtained at low bias voltage. The polarization effects of the molecule are negligible in this case,[20] and the staircase like $I(V)$ characteristic of the junction at large bias voltage will not be studied in detail in this paper (see the end of Sec. III).

Connected to two infinite perfect wires, the PMIM junction can be considered as an impurity compared to the periodic atomic structure of the connecting wires. The most elementary characteristic of the electronic scattering properties of this impurity are the $[t]$ transmission and $[r]$ reflection matrices connecting the incident flux of electrons on one side of the PMIM junction to the outgoing flux on the other side. The low bias voltage conductance of the PMIM junction is given by the generalized Landauer formula[21,22]

$$G = \frac{e^2}{\pi\hbar}T(E_f) = \frac{e^2}{\pi\hbar}\mathrm{Tr}([t(E_f)][t(E_f)]^+). \qquad (2)$$

Different methods are used to calculate the transmission matrix $[t]$. The scattering matrix can be calculated from the spatial propagator associated with the Schrödinger equation[23] or, from its kernel, the Green function.[13,24] In this last method, the two electrodes appear as jellium ''connected'' to the discrete levels of the molecular wire via a Lorentzian- or Gaussian-like enlargement of each molecular levels.[24] This greatly simplifies the calculations, but the description of the contact resistance between the wire and the pads is lost.

Here, the matrix $[t]$ is calculated using the ESQC (electron-scattering quantum chemistry) technique. In ESQC, the multichannel spatial propagator is built starting from the projection of the pad-molecule-pad Hamiltonian on a lowest combination of atomic orbitals basis set. This opens the way to use a quantum-chemistry description of the PMIM junction. This technique was used with success to calculate STM images[25] and the conductance of small molecules like C_{60} in very good agreement with experimental results.[1] For large molecules, only the extended Hückel molecular orbital (EHMO) method can be used to construct the PMIM-Hamiltonian. Self-consistent calculation may be performed to improve it, but a prohibitive calculation time would arise in this case. Already, each atom of the junction is described in ESQC by its full valence structure with Slater orbitals and spatial overlap calculated exactly between all the atoms of one cell and between a cell and its nearest neighbors.[26]

The atomic structure of the PMIM junction chosen is given in Fig. 2. The unit cell of the electrodes is a slab of 8×6 gold atoms in section with the (110) face perpendicular to the tunnel current propagation (Oz). In this case, only two layers of gold atoms are necessary to reconstruct the full fcc gold lattice. With this choice and with only a $6s$ orbital per Au atom the maximum order of $[t]$ is 96. On each side, the PMIM junction is made of a unit cell prolongated by a pad of 8×4 Au atoms in section and four Au atoms in length. This reduction of the electrode section allows the definition of (001) surfaces per pad, where each end of the molecule will be adsorbed. The advantage of such a surface on the pad is that different adsorption sites can be explored to optimize the contact resistance. As the adsorbed ends of each molecule are different from one to another, the length considered in all calculations is the pad-pad distance and not the exact length of the oligomers. The chemisorption altitudes for the molecular wire at both ends had been frozen at 2.0 Å, which is the equilibrium distance of a benzene molecule on a metallic surface,[27] but other altitudes have also been explored. Before its chemisorption, the conformation of the oligomer was optimized. Since elementary conformation changes on the oli-
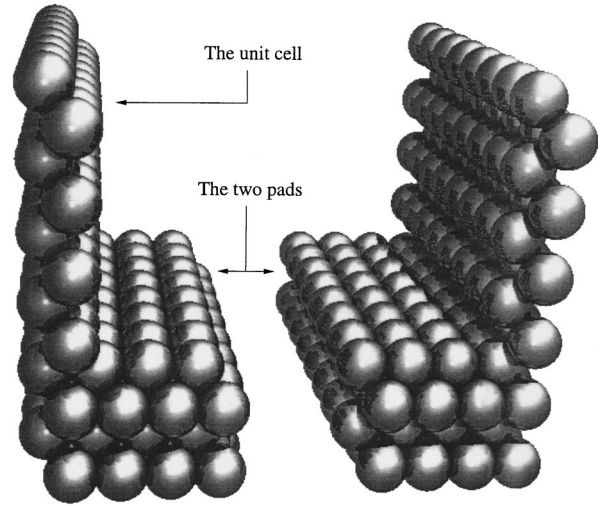

FIG. 2. A view of the atomic structure of the PMIM junction used. This junction is connected on each side to an electrode unit similar to the periodic cell.

gomer are known to modify G,[13] a planar conformation was forced for all the oligomers studied for the sake of comparison between them. But any conformation of the oligomers can also be calculated.

A first step before calculating G for a pad-molecule-pad junction was to be sure that the conductance of a pad-vacuum-pad junction is well calculated, with a ''conductance-pad separation'' characteristic in agreement with the exponential law known experimentally for such a junction. Furthermore, the tunneling current through space must be small enough in comparison with the tunnel current through the molecular wire. At sufficiently large pads separation and for a given Fermi energy, for a metal-vacuum-metal tunnel junction[28] the WKB approximation gives

$$T(E_f,d) = \mathrm{Tr}([t(E_f,d)][t(E_f,d)]^+) = \frac{2K_0}{8\pi d}e^{-2K_0 dS^*},$$
$$(3)$$

where S^* is the section of the pads, d the inter-pads distance and $K_0 = \sqrt{2m\phi}/\hbar$ with ϕ the metal work function.

With the ESQC technique, the WKB law is retrieved for large d by using a simple ζ basis set of $6s$ orbitals in the bulk and a double-ζ basis set of the same orbital for the surface Au atoms on the pads (Fig. 3). Notice that the double ζ parametrization was optimized to recover the 5.1-eV work function of gold. At small distance, it is known that the tunnel barrier collapses.[29] In that case the tunnel current saturates to reach the maximum conductance at contact. Therefore, the variations of $T(E_f,d)$ with d must deviate from Eq. (3) and saturate as shown by calculation (Fig. 3).

III. OLIGO(THIOPHENE ETHYNYLENE)'S

Among the oligomers listed in Table I, we have chosen the oligo(thiophene ethynylene)'s to study in detail the tun-
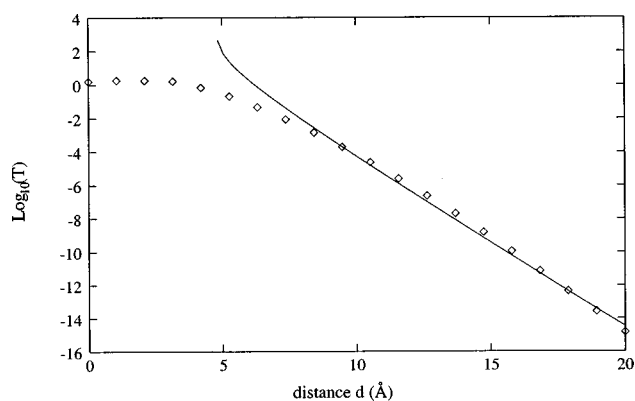
FIG. 3. Variations of $T(d)$ as a function of the distance d between the two gold pads. The straight line is a plot of the WKB variations calculated with Eq. (3), while the diamonds represent the ESQC calculation. All parameters were calibrated to reproduce the WKB results at large distance. A saturation occurs at a short distance not reproduced by the WKB approximation.

nel phenomenon through a molecular wire of definite length. A (thiophene ethynylene) oligomer is a conjugated linear molecule with an alternation of double and triple bonds. Along this oligomer, the double bonds are stabilized in thiophene ring structures. The triple bonds offers the advantage that a local oligomer conformation change will not completely destroy the conjugation. This is the reason why Tour proposed this conjugated skeleton as a prototype of molecular wire.[11] This will be an advantage in using such oligomer as a jumper over a PMIM junction.

An oligomer of 9-thiophene rings (Fig. 4) with a length of 52.51 Å was chosen for this study. Its electronic structure is composed of 309 molecular orbitals, 79 of the π type and 185 of the σ type (plus 45 diffusive d orbitals to describe the doublet of the sulfur atoms). A close look at the molecular-orbital structure shows that the HOMO and LUMO are π delocalized over all the oligomer skeletons, but with specific node distributions which will play a role in the determination of the active tunneling channel through this oligomer. Adsorbed between the electrodes as described in Fig. 1, this oligomer will stabilize a tunnel current in the circuit. Three contact geometries have been considered: (a) Each end thiophene of this 9-oligomer is chemisorbed on a PMIM electrode (100) face with a 2-Å altitude. The electrode-electrode separation is $d=49.6$ Å in this case. (b) The 9-oligomer is physisorbed perpendicular to the (110) face of the electrode. (c) A sulfur atom is introduced at each end of the 9-oligomer in (b) to improve the contact conductance. In these two last cases, the electrode-electrode distance is $d=61.1$ Å. As expected, the PMIM conductance is highly enhanced by the introduction of the conjugated oligomer. In case (a), the current intensity $I=0.13$ pA for a 0.1-V bias voltage. This must be compared with current intensities orders of magnitude lower than the attoampere for the same
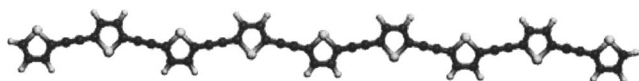

FIG. 4. Ball and stick representation of the 9-thiophene molecule. Only one ring at each end is adsorbed on the first pad site.
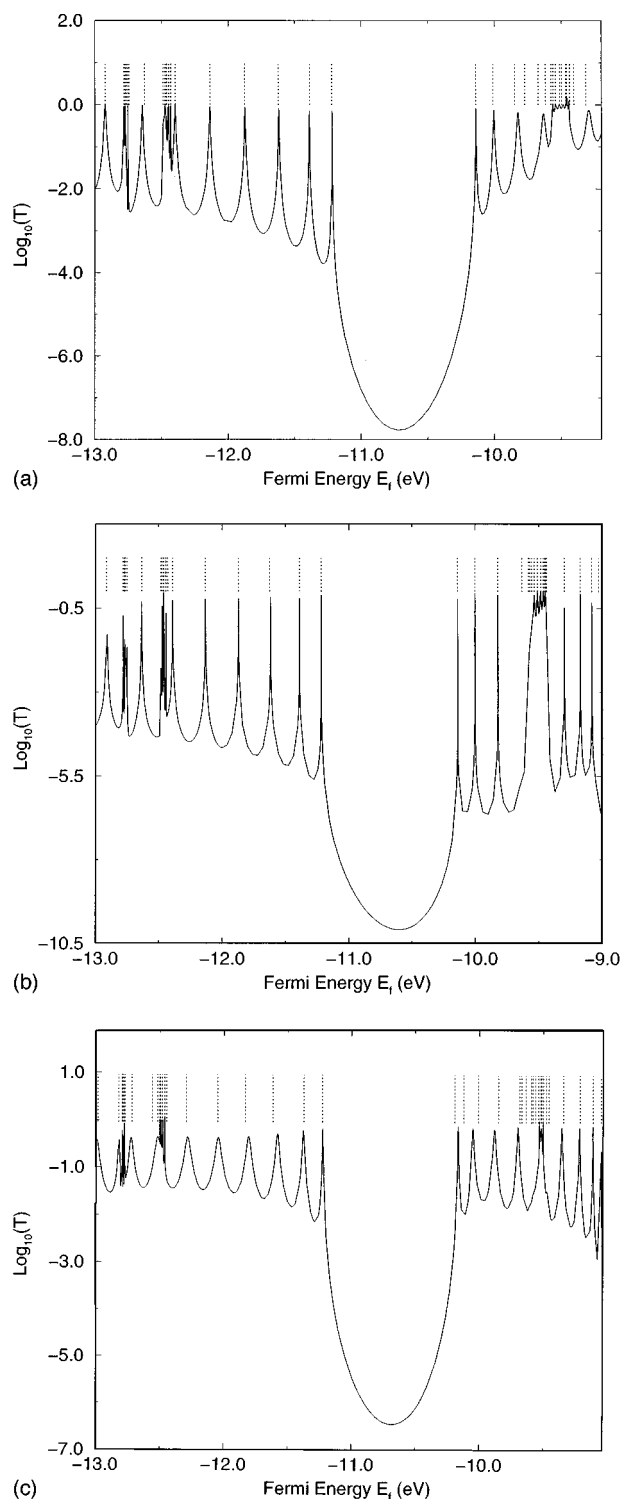

FIG. 5. Three $T(E)$ spectra of the oligo(thiophene ethynylene) molecule corresponding (a) to the π position, (b) the σ position with the sulfur atoms, and (c) without it. The dashed lines represent the molecular level positions.

electrode-electrode separation but without the molecule.

Electronic tunneling spectra of this junction are presented in Fig. 5 for each adsorption configuration. Those spectra are obtained by calculating $T(E)$ in Eq. (2) using the ESQC-EHMO technique for a given energy range. Experimentally, such spectra can be obtained by plotting $(dI/dV)/(I/V)$ characteristics as a function of the bias voltage V. In one part

of the spectrum, there are no resonances, as they accumulate aside from it. Each resonance can be associated with a given oligomer molecular level. The accumulation of the resonances with an increase of the oligomer length will form the band structure of the infinite molecule. In particular, parts of the represented resonance will enter into the formation of its valence and conduction bands. The nonresonant central part of each spectrum corresponds to the HOMO-LUMO gap of the oligomer. Its paraboloïd shape can be approximated by an argument due to Franz, quoting that the simplest way to link valence and conduction bands is via a paraboloïd in a complex wave-vector approach.[30] The tunneling transport regime occur in this paraboloïd part of the spectrum for a bias voltage lower than the HOMO-LUMO gap of the oligomer. Ballistic transport regime will occur in the resonant parts of the spectrum for a long enough wire in such a way that the peak to peak separation is lower than kT.

As in a standard double-barrier model, the width of each resonance is a function of the interactions between the discrete 9-oligomer orbitals and the two electrodes electronic states. Each resonance is a Lorentzian enlarged by these interactions.[31] Looking at the resonance width, which are larger for (c), intermediate for (a), and small for (b), we retrieve the expected comparisons of the interactions between (a) the chemisorbed case and (b) the physisorbed one, and we can establish the enhancement due to the presence of the sulfur atoms in case (c). The last remark opens the way to lowering the contact resistance of the wire-pad connection by modifying the internal end structure of the molecule (see Sec. IV).

It is also important to identify the molecular levels contributing to the tunnel transport regime in the HOMO-LUMO gap. At a given energy E_c, a tunnel channel is opened if the tail of a resonating level, even far away from E_c, is non-negligible in the gap. It is the superposition of all these channels which gives the HOMO-LUMO paraboloïd. However, not all the molecular levels contribute to it, and the superposition of the contributing ones may be constructive or destructive. The identification of tunneling channels can be performed by canceling oligomer molecular levels one after the other when calculating $T(E)$ to determine which are necessary. To suppress the contribution of a level $|\psi_i\rangle$ to the tunneling current, the Hamiltonian and the overlap matrices used in the EHMO to describe the PMIM electronic structure are projected on a subspace of the PMIM states generated without $|\psi_i\rangle$. Then the scattering matrix is calculated as usual on this subspace. This can be applied systematically for a small molecule,[1,25] but all combinations cannot be tested on our large oligomers made of 309 levels or more.

To identify the tunneling channels for the adsorption configuration (a) the σ levels of the molecule were first suppressed, resulting in no changes in the paraboloïd. Furthermore, π levels which are not overlapping with the two electrodes were also suppressed, plus the π levels with an energy far away from the HOMO and LUMO levels. Proceeding this way, the active subspace reduces form 309 orbitals to 42, with no notable change in the central paraboloïd (Fig. 6). This determines the 42 tunnel channels supporting the tunnel current through the 9-oligomer. Thirty-three of them are from the HOMO side and nine from the LUMO side. The orbital decomposition of these 42 channels shows
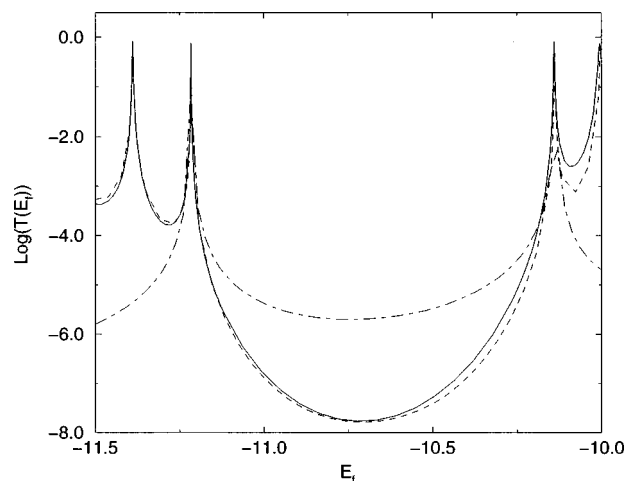

FIG. 6. $T(E)$ spectra of the 9-thiophene [with configuration (a)] depending on the number of molecular orbitals activated. The straight line is the real spectrum, calculated with all 309 orbitals activated. The dashed line is a plot with only 42 channels activated. All these channels are of π symmetry, with an energy between -15.3 and -9.0 eV. The dot-dashed line is a plot with only HOMO and LUMO states considered.

that each one possesses at least one significant weight on the atoms at both ends of the molecule. Notice that if only the HOMO and LUMO of the 9-oligomer is kept, the original paraboloïd is not at all reproduced (Fig. 6). This demonstrates that the tunnel regime results from a complex superposition of tunnel channels. In the (b) and (c) cases, a decomposition can be made in the same way. Differences arise from the contribution of σ levels due the adsorption configuration of the oligomer.

Finally, the $I(V)$ characteristic of the PMIM junction closed by the 9-oligomer can be calculated using the $T(E)$ spectra and the following equation:[32]

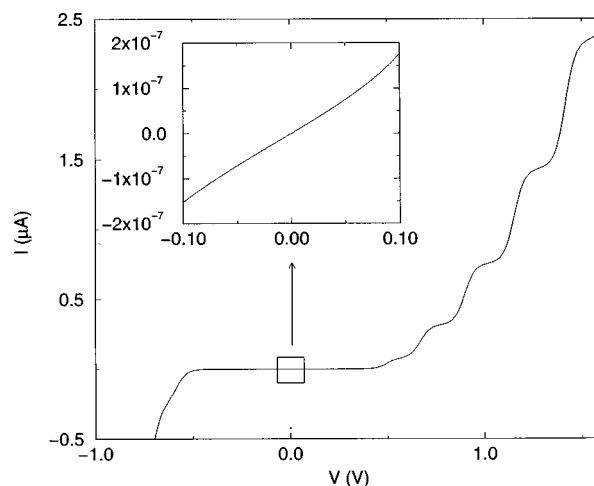$$I(V) = \frac{e^2}{\pi\hbar} \int_{-\infty}^{+\infty} T(E)[f_1(E+eV) - f_2(E)]dE, \qquad (4)$$

FIG. 7. A calculated $I(V)$ characteristic for the 9-thiophene oligomer. This curve was plotted using the spectrum in Fig. 5(a) for a temperature $T = 300$ K.

with f_1 and f_2 the Fermi-Dirac functions in the two electrodes.

The $I(V)$ plot for the adsorption configuration (a) is given in Fig. 7 for a temperature of 300 K. For high voltage, the $I(V)$ looks like a Coulomb blockade curve but is not, since the steps sizes are not regular. As the polarization effects were neglected, we cannot detail more greatly these parts of the curves. Nevertheless, it is important to notice its staircase behavior, simply due to the large energy distance between each resonance of the $T(E)$ spectrum.[33] For each bias voltage increase reaching another molecular level or set of levels, a step results on the $I(V)$ curve. At low bias voltage, a zoom shows the linear $I(V)$ part of the characteristics corresponding to the tunnel transport regime. This linearity is the principal reason to study tunneling transport regime in the gap range, although the transmission coefficient is small through the 9-oligomer and decreases with its length.

IV. EXPONENTIAL LAW

In Sec. III, the importance of a detailed study of the HOMO-LUMO energy range of a molecular wire was shown. In this gap, the transport regime through the molecular wire is tunneling leading to the exponential decrease of the junction conductance with the length of the wire (1). Compared with Eq. (3), the difference is that the inverse damping length γ in the wire is no longer controlled by the metal electrode work function but by the intrinsic electronic properties of the molecule. Notice that Eq. (1) can be demonstrated analytically for families of tight-binding chains,[34] and was recovered on simple oligomers.[14]

A. Damping factor γ

For the series of oligomers presented in Table I, it is not possible to recover Eq. (1) analytically. Only lengthy numerical calculations permit one to plot the conductance variations with the oligomer length for long molecules. Since we are interested in the exponential law in the HOMO-LUMO gap, the plots were calculated for each oligomer and each length at the minimum in energy of the $T(E_f,d)$ curve in this gap. The length considered is the electrode-electrode distance d after the adsorption of oligomers at both ends. One can also consider the exact oligomer length, but the adsorbed ends are different from molecule to molecule. Therefore it is preferable to take into account these differences in γ for a better comparison. As expected, each class of oligomer produces a specific exponential decrease of the junction conductance with length d (Fig. 8). The corresponding calculated damping factor γ is reported in Table I.

It is usually assumed that γ is only a function of the HOMO-LUMO gap of the oligomers considered.[13] This is an extension of the known two-band model of tunneling through a junction made of an insulator or a semiconductor.[35] However, we have demonstrated that this extension is not valid since all the electronic structures of the oligomer contribute to γ.[14,34] This is shown in Fig. 9, where E_g, the gap of the wire, is plotted as a function of γ. In each case the gap was evaluated by considering an infinite long oligomer per family to stabilize the HOMO-LUMO gap variations with length. Although a tendency from this curve
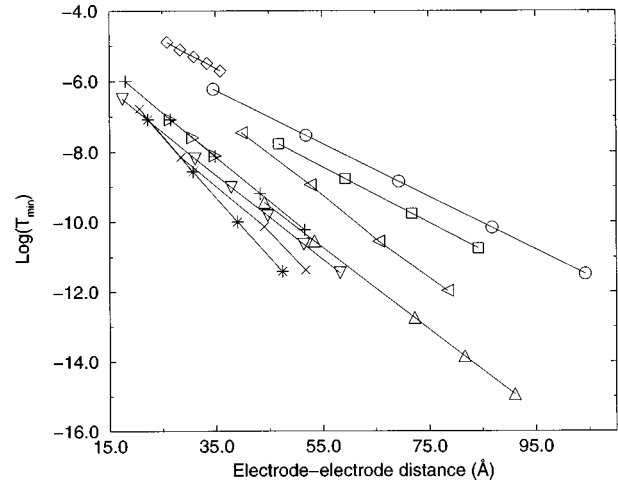

FIG. 8. Variations of $T(E)$ as a function of the electrode-electrode distance for a large number of oligomers. The $T(E)$ values reported are the minimal ones in the gap of each molecule. $\bigcirc$ is for oligo(phenylbutadiyne), $\square$ for oligo(thiophene ethynylene), $\diamondsuit$ for oligo(phenylethynylene), $\triangle$ for oligo(cyclopenta-naphto-fluoranthene), $\triangleleft$ for oligo(thiophene butadiyne), $\triangledown$ for Polyenes, $\triangleright$ for oligo(phenyl), $+$ for oligo(pyridophenantridine), $\times$ for oligothiophenes, and $*$ for oligo(benzoanthracene).

is that γ decreases when E_g is small, a large dispersion of γ values can be found for a given gap. This shows that not only E_g contributes to γ but also the detailed electronic structure of the oligomer. Our oligomers are made of a repetition of monomer units. The atomic orbitals of a unit are involved in a large number of oligomer molecular orbitals which do not always belong to the conduction or valence band in formation. Therefore, the $T(E)$ paraboloïd in the HOMO-LUMO gap is dependent on the position of the oligomer band structure obtained when its length goes to infinity. Furthermore, the evolution of this paraboloïd with an increase of the number of units in the oligomer is dependent on the details of the destructive and constructive inter-
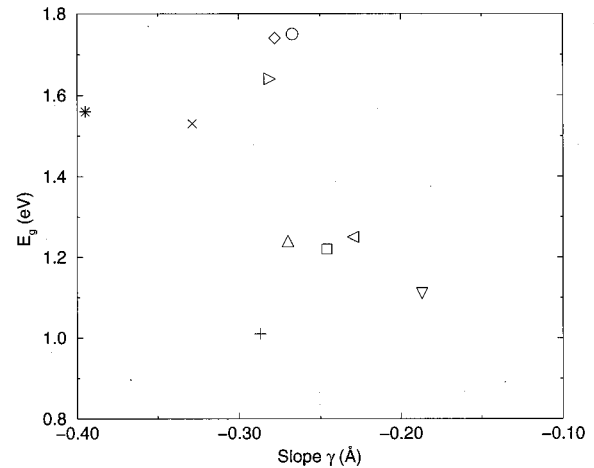

FIG. 9. Variations of E_g as a function of γ for all the molecules. $\bigcirc$ is for oligo(phenylbutadiyne), $\square$ for oligo(thiophene ethynylene), $\diamondsuit$ for oligo(phenylethynylene), $\triangle$ for oligo(cyclopenta-naphto-fluoranthene), $\triangleleft$ for oligo(thiophene butadiyne), $\triangledown$ for Polyenes, $\triangleright$ for oligo(phenyl), $+$ for oligo(pyridophenantridine), $\times$ for oligothiophenes, and $*$ for oligo(benzoanthracene).
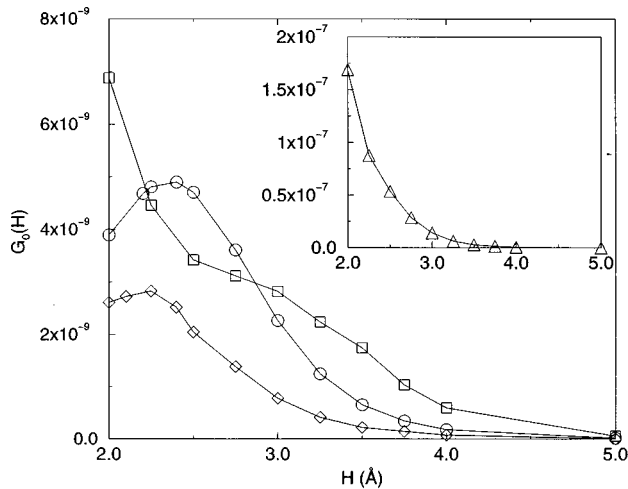
FIG. 10. Variations of the prefactor G_0 with the height H of the molecule above the gold pads. $\bigcirc$ is for oligo(phenylbutadiyne), $\square$ for oligo(thiophene ethynylene), $\diamond$ for oligo(phenylethynylene), and $\triangle$ for oligo(cyclopenta-naphto-fluoranthene).

ferences of the electrons tunneling from one unit through another along the oligomer. This means that a small γ will be given by a unit whose reflection and transmission have been well adapted all along the wire. This adaptation, reminiscent of an impedance adaptation in microwave technology, may not have to be regular all along the oligomer. The complex dependence between γ and E_g is exemplified in two cases. In the oligo(phenyl), oligo(phenylethynylene), and oligo(phenylbutadiyne) series, adding a triple bond decreases γ at each step, but E_g increases at the same time. Conversely, going from the oligo(benzoanthracene) to the oligo(pyridophenantridine) decreases γ and E_g at the same time. This shows the need for a detail optimization of the oligomer unit to take benefit of a small γ for a large E_g. Such an E_g is required since the molecular electronic structure has to be preserved in interacting with the pads. Further-
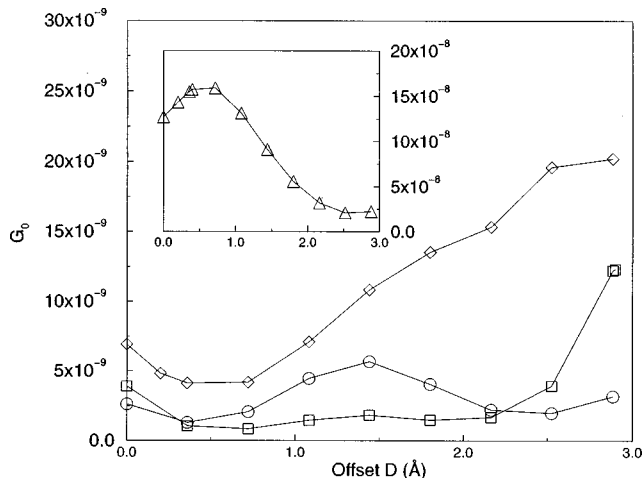

FIG. 11. Variations of the prefactor G_0 with the offset D on the surface. An offset of 0.0 Å corresponds to a hollow site, while an offset of 2.884 Å corresponds to the next hollow site. $\bigcirc$ is for oligo(phenylbutadiyne), $\square$ for oligo(thiophene ethynylene), $\diamond$ for oligo(phenylethynylene) and $\triangle$ for oligo(cyclopenta-naphto-fluoranthene).

TABLE II. Change in the pad-molecule-pad characteristics γ and G_0 as functions of the oligomer end for the oligo(phenylethynylene)'s.

End type	γ	$\frac{\pi \hbar}{e^2} G_0$
	0.278	3.95×10^{-5}
	0.277	8.24×10^{-4}

more, the tunneling $I(V)$ curves can be kept linear and temperature independent over a large bias voltage range.

B. Contact conductance G_0

From detailed calculation on tight-binding systems[14,34] it is known that G_0 in Eq. (1) depends on the electronic interactions between the extremity of the oligomer and each pad. Therefore it is important to optimize G_0 by a good choice of the adsorption site of the oligometer ends, and by an optimization of the chemical composition of these ends. We have therefore systematically changed the adsorption position of the oligomer ends to follow the G_0 variations. Notice that in all positions studied γ was recalculated, and remains unchanged for a given oligomer family. This confirms the role of γ and G_0: γ is characteristics of the internal structure of the oligomer, and g_0 of the contact with the pads.

Two variations of the adsorption configurations were studied for the optimization of G_0. Starting from the chemisorption position of each oligomer where the π tunnel channels are active (see Sec. III), the altitude of the adsorbed ends above the pads was changed (Fig. 10). A lateral shift of these ends was also studied to check the specificity of the chemisorbed site of the oligomer and how G_0 increases depending on the site chosen (Fig. 11). Notice that both ends were changed simultaneously, since an asymmetry in the connection will decrease G_0 by the creation of an asymmetric effective tunneling barrier.

The two possibilities of changing the adsorption configuration bring the same conclusions: improving G_0 is rather difficult this way. Changing the lateral position is a good way to optimize the interactions of the molecular orbitals at the ends of the oligomer with the metal. But this cannot account for more than a multiplication by factor 2 or 3 of G_0. For each adsorbate and each length an optimum altitude and adsorption site exists to create a maximum of constructive superposition of π channels, but the gain on G_0 is limited.

Another way to improve G_0 is to change the molecular-orbital repartition at the oligomer ends by changing their chemical compositions compared to the oligomer unit. We tested this possibility on the oligo(phenylethynylene) molecule (see Table II). A multiplication by a factor 20 of G_0 was obtained simply by changing the benzene groups at the ends of the molecule by anthracene groups. This is a proof that by changing the π electron distribution on the oligomer

and at its ends, one can gain much on G_0: the contact barrier decreases due to a better orbital mixing between the two contact partners.

Notice also that the results reported in Table I permit an evaluation of the net current through the junction as it would be measured for each oligomer for a pad-pad separation of 8 nm and a 0.1 bias voltage. Even with the ''best oligomer'' the current is still too low to be detected. Fortunately we now have two ways to enhance the current: by optimizing G_0 through the design of the wire end, and by enhancing γ with a better design of the oligomer unit.

V. CONCLUSION

Using the ESQC technique, the conductances of many molecular wires have been calculated. The tunneling phenomenon through a molecular wire relies on two parameters: the damping factor γ and the contact conductance G_0. Based on these two parameters, a classification of the molecular wires was given. This allows a better understanding of the tunnel transport phenomenon through a tunnel barrier modified by a molecule. In particular, the molecular orbitals that effectively create the tunnel channels can be separated from the others, bringing out the necessity of a structural adaptation of the molecular wire. This is reminiscent of the impedance adaptation in microwave technology.

I-V characteristics of a molecular wire were calculated, showing a staircase form for high voltage. This is not a Coulomb blockade *I-V* but a consequence of the form of the $T(E_f)$ spectrum. The low voltage part of the curve shows a linear behavior, but for a current smaller than the pA. This means that none of the molecules studied can be fully exploited as wires. The principal reason is their large HOMO-LUMO gap. Some carbon nanotubes can be fabricated with very small gaps and used as nanowires. But the used of oligomers of well-defined length is still more promising because it permits the synthesis of nanodevices by including the chemical functionality in the wire. There are two possibilities for optimizing these molecules: enhancing γ by a change in the internal structure of the molecules, and increasing the contact conductance G_0 by an optimization of the molecular wire ends.

[1] C. Joachim, J. K. Gimzewski, R. R. Schlitter, and C. Chavy, Phys. Rev. Lett. **74**, 2102 (1995).

[2] A. Yazdani, D. M. Eigler, and N. D. Lang, Science **272**, 1921 (1996).

[3] C. Joachim and J. K. Gimzewski, Europhys. Lett. **30**, 409 (1995).

[4] J. T. Sander, M. H. Devoret, H. Dai, A. Thess, R. E. Smalley, L. J. Geerligs, and C. Dekker, Nature **386**, 474 (1997).

[5] N. D. Lang, Phys. Rev. B **52**, 5335 (1995).

[6] A. D. Schlüter, M. Löffler, and V. Enkelmann, Nature (London) **368**, 831 (1994).

[7] J. M. Tour and J. J. S. Lamba, J. Am. Chem. Soc. **115**, 4935 (1993).

[8] J. S. Schumm, D. L. Pearson, and J. M. Tour, Angew. Chem. Int. Ed. Engl. **33**, 1360 (1994).

[9] D. Pearson, J. Schumm, and J. Tour, Macromolecules **27**, 2348 (1994).

[10] W. Hoeve, H. Wynberg, E. E. Hyavinge, and E. W. Meijer, J. Am. Chem. Soc. **113**, 5887 (1991).

[11] J. M. Tour, Chem. Rev. **96**, 537 (1996).

[12] J. Roncali, Chem. Rev. **97**, 173 (1997).

[13] M. P. Samanta, W. Tian, and S. Datta, Phys. Rev. B **53**, R7626 (1996).

[14] C. Joachim and J. F. Vinuesa, Europhys. Lett. **33**, 635 (1996).

[15] B. Mahn and H. Kuhn, J. Appl. Phys. **42**, 4398 (1971).

[16] M. Magoga and C. Joachim (unpublished).

[17] R. P. Andres, T. Bein, M. Dorogi, S. Feng, J. I. Henderson, C. P. Kubiak, W. Mahoney, R. G. Osifchin, and R. Reifenberger, Science **272**, 1323 (1996).

[18] J. W. Mintmire, B. I. Dunlap, and C. T. White, Phys. Rev. Lett. **68**, 631 (1992).

[19] V. Rousset, C. Joachim, S. Itoua, B. Rousset, and N. Fabre, J. Phys. (France) III **5**, 1983 (1995).

[20] D. Lamoen, P. Ballone, and M. Parinello, Phys. Rev. B **54**, 5097 (1996).

[21] M. Büttiker, Y. Imry, R. Landauer, and S. Pinhas, Phys. Rev. B **31**, 6207 (1985).

[22] A. D. Stone and A. Szafer, IBM J. Res. Dev. **32**, 384 (1988).

[23] J. Stein and C. Joachim, J. Phys. A **20**, 2849 (1987).

[24] V. Mujica, M. Kemp, and M. A. Ratner, J. Chem. Phys. **101**, 6849 (1994).

[25] P. Sautet and M. L. Bocquet, Phys. Rev. B **53**, 4910 (1996).

[26] C. Joachim, *Scanning Probe Microscopy: Beyond the Images* (Edition de Physique, Paris, 1992), p. 91.

[27] M. Abon, J. C. Bertolini, J. Billy, J. Massardier, and B. Tardy, Surf. Sci. **162**, 395 (1985).

[28] J. G. Simmons, J. Appl. Phys. **34**, 1793 (1963).

[29] J. K. Gimzewski and R. Möller, Phys. Rev. B **36**, 1284 (1987).

[30] W. Franz, *Handbuch der Physik* (Verlag Julius Springer, Berlin, 1956), Vol. 17, p. 155.

[31] W. Xue and P. A. Lee, Phys. Rev. B **38**, 3913 (1988).

[32] R. Landauer, Physica D **38**, 226 (1989).

[33] M. Kemp, V. Mujica, and M. A. Ratner, J. Chem. Phys. **101**, 5172 (1994).

[34] M. Magoga and C. Joachim, Europhys. Lett. (to be published).

[35] K. H. Gundlach, J. Appl. Phys. **44**, 5005 (1973).